Available online at www.sciencedirect.com
SCIENCE DIRECT
Journal of Catalysis 234 (2005) 111–118
JOURNAL OF CATALYSIS
www.elsevier.com/locate/jcat

Determination of the catalytically active oxidation Lewis acid sites in Sn-beta zeolites, and their optimisation by the combination of theoretical and experimental studies

Mercedes Boronat, Patricia Concepción, Avelino Corma *, Michael Renz, Susana Valencia

Insitituto de Tecnología Química, UPV-CSIC, Avda. los Naranjos s/n, 46022 Valencia, Spain

Received 17 March 2005; revised 17 May 2005; accepted 26 May 2005

Available online 14 July 2005

Abstract

Two types of Lewis acid sites are shown to exist in Sn-beta zeolite: partially hydrolysed framework tin centers $(–Si–O–)_3Sn–OH$ (sites A) and fully framework coordinated tin atoms $Sn(–Si–O–)_4$ (sites B). ONIOM and DFT calculations for adsorbed acetonitrile, which is a probe molecule for Lewis acid sites, show that acetonitrile coordinates more strongly to partially hydrolysed framework Sn (sites A) in Sn-beta zeolite than to nonhydrolysed framework Sn (sites B). The corresponding IR bands associated with the $\nu(C{\equiv}N)$ stretching vibration were also calculated. Adsorption–desorption experiments of deuterated acetonitrile on Sn-beta give two IR bands at 2316 and 2308 cm^{-1} with IR shifts of 43 and 51 cm^{-1} with respect to gas-phase acetonitrile. These values are in excellent agreement with theoretical calculations, making it possible then to associate the Lewis sites related to 2316 and 2308 cm^{-1} with partially hydrolysed and nonhydrolysed framework Sn sites, respectively. Catalytic results confirm that partially hydrolysed Sn (sites A) is much more active than fully framework-integrated Sn (sites B) for Baeyer–Villiger oxidation of cyclic ketones. Finally, the ratio between these two types of sites could be influenced by postsynthesis treatments.

Keywords: Sn-beta; DFT calculations; IR spectroscopy; Lewis acidity; Acetonitrile adsorption; Baeyer–Villiger; Deep and shallow bed calcinations

1. Introduction

Sn-beta zeolites are active catalysts for oxidation of cyclic ketones and aromatic aldehydes with hydrogen peroxide [1–4], Meerwein–Ponndorf–Verley (MPV) reductions, Oppenauer oxidations [5,6], and the Carbonyl–Ene cyclisation of citronellal to isopulegol [7]. The principal activation has been attributed to a coordination of the carbonyl group to the Lewis acidic tin centre involving a polarisation of the carbonyl group and entailing a more electrophilic carbonyl carbon atom. As a consequence, this carbon atom can now be attacked by weak nucleophiles like hydrogen peroxide [1–4] or "hydride species" [5,6] or by a simple double bond [7], yielding the esters, lactones, and alcohols, respectively. The first theoretical studies on tin-catalysed Baeyer–Villiger reactions of ketones were done with a small $Sn(OH)_4$ cluster to simulate the active site [8]. A more recent theoretical simulation of the tin centre incorporated into a siliceous matrix (zeolite beta) combined with a kinetic study revealed that in addition to the Sn Lewis-acid site, the basic oxygen adjacent to the tin centre also plays an important role by adsorbing H_2O_2 in the Baeyer–Villiger oxidation [9].

During the interaction between the carbonyl group and the Sn site, the electron density transferred to the tin centre is localised in the lowest unoccupied molecular orbital (LUMO) that is a combination of the four $\sigma^*_{Sn–O}$ antibonding orbitals. As a consequence, the $Sn–O_{framework}$ bond lengths should increase. Since the rigidity of the zeolite structure makes this difficult, a relaxation of the framework by the hydrolysis of a Sn–O–Si bridge should facilitate the

* Corresponding author.
E-mail address: acorma@itq.upv.es (A. Corma).

0021-9517/$ – see front matter
doi:10.1016/j.jcat.2005.05.023

reaction by generating a $(–Si–O–)_3Sn–OH$ site. Such a hydrolysis is not uncommon in other zeolites [10,11] containing framework metal sites and could also very well occur in Sn-beta. If this is the case, one could expect partially hydrolysed Sn sites (sites A) to be more active than nonhydrolysed framework Sn (sites B). In the case of Ti-zeolites, for example, it has been shown that $Ti(OSi)_3OH$ centers are present in TS-1 [12] and that they are more reactive for propylene epoxidation than fully coordinated Ti sites [13]. Furthermore, the relative concentrations of both types of sites in Sn-beta should depend on catalyst postsynthesis treatment.

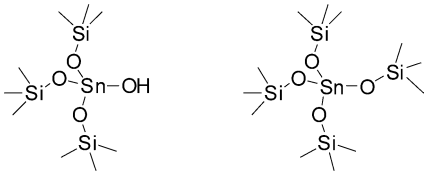

The present work first shows by theoretical calculations that the adsorption of a probe molecule for Lewis acid sites, such as deuterated acetonitrile, is favoured on partially hydrolysed framework Sn (site A) with respect to site B. Acetonitrile has been selected since it is very sensitive to different coordination spheres of the metal centre and it can be monitored easily by IR spectroscopy. Indeed, it will be seen that the theoretical calculations are confirmed by IR spectroscopic results of deuterated acetonitrile adsorption–desorption on Sn-beta zeolite, which shows the presence of two Lewis (Sn) sites that retain acetonitrile with different strengths and whose relative adsorption frequencies correspond with those calculated theoretically for sites A and B. Finally, catalyst treatment under different reaction conditions dramatically changes the ratio of these two types of Lewis acid sites, and the catalytic activity for the Baeyer–Villiger oxidation directly correlates with the concentration of sites A.

2. Experimental

2.1. Computational details

The nine crystallographic positions existing in beta zeolite can be classified into three groups according to their connectivity: T1 and T2 are associated with one four-membered ring; T3, T4, T5, and T6 occupy a vertex of two four-membered rings; and T7, T8, and T9 are associated with no four-membered rings. Since the geometry of the T positions belonging to the same group are quite similar, only one crystallographic position representative of each group has been considered in the theoretical study: T1, T5, and T9.

For each one of the three T positions considered, a cluster containing the T atom and four coordination spheres around it was cut out from the periodic structure of pure silica beta zeolite [14], and the dangling bonds that connected the cluster to the rest of the solid were saturated with H atoms at 1.49 Å from the Si atoms and oriented towards the positions occupied in the crystal by the oxygen atoms in the next coordination sphere. The Si atom in the T position of each cluster was replaced by Sn, and one CH_3CN molecule was adsorbed on it. We simulated the hydrolysis of a Sn–O–Si bridge by deleting one Si atom from the model and saturating with H atoms the corresponding dangling bonds. All different Sn–O–Si bridges were hydrolysed for each T position considered, but only the results for the most stable system are reported. For the sake of comparison, the coordination of acetonitrile to an isolated silanol defect site ($CH_3CN–Si_4O_4H_{10}$) was also included in the study and was simulated with a smaller model. The resulting models for Sn-beta are depicted in Fig. 1, and the model for the silanol group is shown in Fig. 2.

In a first series of calculations (named ONIOM), the geometries of all of the zeolite–CH_3CN complexes considered in this study and of the zeolite models without the adsorbate were optimised by means of the ONIOM scheme [15,16] as implemented in the Gaussian 03 computer program [17]. The ONIOM approach subdivides the *real* system into several parts or layers, each of which is described at a different level of theory. The most important one is called the *model* system and is described at the highest level of theory, whereas subsequent layers are computed at progressively lower and computationally cheaper levels of theory. In the ONIOM approach, the total energy of a system subdivided into two layers is approximated as

$$E^{\mathrm{ONIOM}} = E(\mathrm{high,model}) + E(\mathrm{low,real}) - E(\mathrm{low,model}).$$

In the present work, the model system includes the Sn atom, the four O atoms in the first coordination sphere, the Si or H atoms bound to them, and the acetonitrile molecule. The coordinates of these atoms were completely optimised with the density functional B3PW91 method [18,19] (DFT), a LANL2DZ effective core potential basis set for Sn [20], and the standard 6-31G(d,p) basis set [21] for N, C, O, Si, and H atoms. The rest of the system was treated at the semiempirical MNDO level, and only the coordinates of Si and O atoms were optimised.

In order to improve the calculated frequency shifts that should be compared with experimental data, in a second series of calculations (named DFT), the geometries of the zeolite–CH_3CN complexes B-T1, B-T5, and B-T9 and of the most stable system with a Sn–OH defect in each T position (A-T1, A-T5, and A-T9) were re-optimised, with all of the atoms treated at the B3PW91 (DFT) theoretical level. The smaller ($CH_3CN–Si_4O_4H_{10}$) model used to simulate the interaction of acetonitrile with an isolated silanol defect site was also optimised at the higher theoretical level (DFT). Frequencies were calculated for both series at the ONIOM level of theory and scaled by 0.9573 as recommended by Scott and

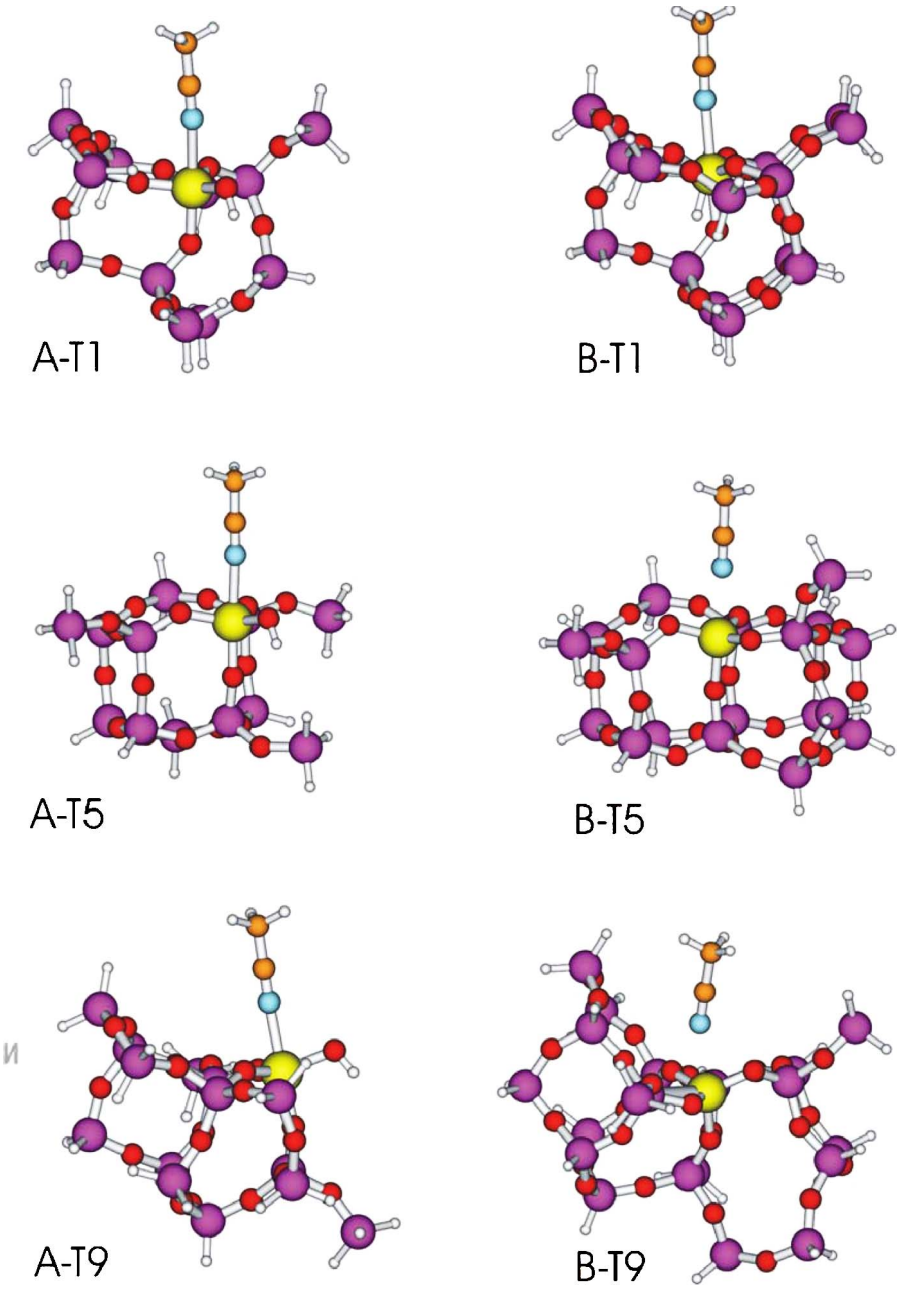

Fig. 1. Structures of the Sn-beta models used in the computational study.

Radom [22]. Orbital energies and occupancies and atomic charges were calculated with natural bond orbital (NBO) methods [23].

2.2. Sample preparation

Two catalyst precursors with different amounts of Sn, namely 1SnB with 1 wt% and 2SnB with 2 wt%, were prepared by hydrothermal synthesis with a procedure described in the literature [2,24]. These materials were activated by calcinations in air at 580 °C for 3 h in an oven. The samples were highly crystalline, and no peaks of SnO_2 were found in the XRD diffractogram or by Raman spectroscopy, indicating that if some of the Sn were in the form of SnO_2, the amount should be very small. Nitrogen adsorption experiments on the calcined beta samples give an isotherm very similar to that of pure silica beta, with a micropore volume of 0.20–0.21 $cm^3\,g^{-1}$ and BET surface areas of 450–475 $m^2\,g^{-1}$. The amount of tin in the samples was determined by atomic adsorption spectroscopy (AAS).

In an alternative activation procedure, we calcined the sample with 2 wt% SnO_2 by a water-saturated air stream into a tubular quartz reactor while heating it from room temperature to 580 °C at 2 °C/min. Then the temperature was kept at 580 °C for 3 h. We controlled the water concentration in the

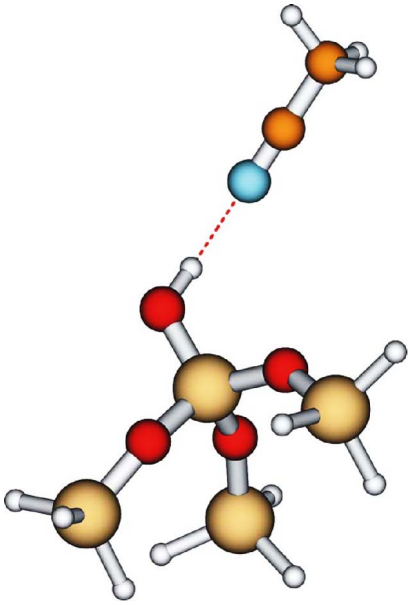

Fig. 2. Structure of acetonitrile adsorbed on a silanol group.

gas stream by passing the air flow through a thermostabilised saturator (e.g., 30 °C) with water or, alternatively, through a water trap. When wet air was used for calcination, the gas flow was changed to dry air during the final cooling period at temperature of 110 °C. Samples involving high catalytic activity were obtained when the air was passed through the saturator at 30 °C (vapour pressure 4.25 kPa) at a flow rate of 20 ml for 150 mg of zeolite sample or at 130 ml for 500 mg. The flow rate has to be increased with the amount of beta catalyst calcined.

For comparative reasons samples prepared by impregnation of a pure-silica beta zeolite with $SnCl_4{\cdot}5H_2O$ (SnO_2B, 2 wt% SnO_2) and by chemical vapour deposition of $SnCl_4$ (CVDSnB, 3.93 wt% SnO_2) were studied. In both cases the samples were calcined at 580 °C for 3 h in a furnace.

2.3. IR experiments

FTIR spectra were recorded with a BioRad FTS-40A FTIR spectrophotometer and a conventional quartz infrared cell connected to a vacuum dosing system. The catalyst powder was pressed into self-supporting wafers (5 mg) and activated at 250 °C in vacuum for 1 h, before the adsorption experiments. Adsorption of deuterated acetonitrile (4–200 mbar) was performed at room temperature with a calibrated volume (1.55 cm^3), followed by time-controlled evacuation at the same temperature. In all cases, FTIR spectra of the unloaded catalyst sample were recorded as reference spectra. IR bands at 2004 and 1880 cm^{-1} on the reference sample were used for normalisation of the spectra. Deconvolution of the IR spectra was done with the ORIGIN software program [25]. For deconvolution, Gaussian-type curves were considered in which the widths of the peaks have been fixed while the peak position was left free.

2.4. Catalytic activity

The Baeyer–Villiger oxidation of adamantanone with hydrogen peroxide was chosen as a test reaction. Five hundred milligrams of adamantanone was mixed with 500 mg of 35% aqueous hydrogen peroxide and 3.0 g of dioxane. A 50-mg sample of the catalyst was added and the reaction mixture was heated to 90 °C for 7 h. The progress of the reaction was monitored by gas chromatography (HP-5 column, 15 m, 0.32 mm, 0.5 µm with an adequate temperature program). A blank experiment showed that conversion in the absence of catalyst can be neglected.

3. Results and discussion

3.1. Theoretical simulation of acetonitrile adsorption

Deuterated acetonitrile has been found to be a suitable molecule for differentiating among Lewis acid sites of different strengths [26–29]. Thus, we have carried out theoretical calculations for the adsorption of acetonitrile on two potential zeolite-beta Sn sites: site A and site B. We disregarded SnO_2 as a potential active site for this study, since reference samples of SnO_2 on silica beta prepared by impregnation did not give any catalytic activity and did not give any IR band due to acetonitrile adsorbed on Lewis acid sites. Furthermore, Sn sites in Sn-beta should correspond to Sn associated with framework positions, because it has been demonstrated by EXAFS and microelectron spectroscopy that these are the most abundant species [30].

For the study of the Sn sites in beta zeolite, three representative models that locate Sn in framework positions T1, T5, and T9 have been considered. The ONIOM results summarised in Table 1 indicate that adsorption of acetonitrile is energetically disfavoured for fully coordinated Sn (sites B) Sn in T1 and is only slightly exothermic in T5 and T9. However, hydrolysis of one of the Sn–O–Si bridges (sites A) facilitates the process, and adsorption energies on site A are between −8 and −9 kcal/mol. The optimised geometry of the complexes and the calculated $\Delta\nu$(C≡N) stretching vibration frequency shifts also indicate a stronger interaction of acetonitrile with site A (Table 1). Thus, the Sn–N distances obtained for site A are between 0.1 and 0.3 Å shorter than those calculated for site B, and the $\Delta\nu$(C≡N) frequency shifts are between 10 and 23 cm^{-1} larger. The reason for this is that Sn in beta zeolite is a Lewis acid that accepts electron density from the acetonitrile molecule. NBO analysis indicates that the primary donor-acceptor interaction between acetonitrile and the Sn Lewis center is a donation from the N lone pair in acetonitrile to a combination of the four σ Sn–O* antibonding orbitals, which is the LUMO (lowest unoccupied molecular orbital) of the catalyst. The change in the occupancies of these orbitals caused by interaction of acetonitrile with the tin center are given in Table 1. It can be seen that the electron density transfer from the N lone pair

Table 1
ONIOM calculated acetonitrile adsorption energies, Sn–N distances, $\Delta\nu$(C≡N) stretching vibration frequency shifts, average variation in the Sn–$O_{framework}$ distances, net atomic charge on acetonitrile and changes in the occupancy of the acetonitrile N lone pair and the catalyst σ(Sn–O)* orbitals caused by acetonitrile adsorption

	E_{ads} (kcal/mol)	rSn–N (Å)	$\Delta\nu$(C≡N) (cm^{-1})	$(\Delta r$Sn–$O_{framework})_{av}$ (Å)	Δq CH_3CN[a] (e)	Δocc. N lone pair[a] (e)	Δocc. σ(Sn–O)*[a] (e)
A-T1	−8.2	2.41	43.1	0.023	0.101	−0.099	0.107
A-T5	−9.2	2.38	51.1	0.021	0.104	−0.101	0.103
A-T9	−9.2	2.38	52.5	0.021	0.107	−0.104	0.101
B-T1	3.0	2.54	32.6	−0.009	0.079	−0.079	0.079
B-T5	−2.3	2.54	36.7	0.016	0.079	−0.078	0.074
B-T9	−0.3	2.64	29.6	0.009	0.066	−0.066	0.067

[a] Results from NBO analysis.

Table 2
Experimental and calculated shifts in the acetonitrile ν(C≡N) stretching vibration frequency. The theoretical values listed are an average of the three values calculated for the three representative sites (T1, T5 and T9)

	Experimental (cm^{-1})	ONIOM (cm^{-1})	DFT (cm^{-1})
Silanol	12	16	16
Site A	51	49[a]	53
Site B	43	33[a]	43

[a] Calculated from the values listed in Table 1.

to the catalyst LUMO is on the order of 0.07–0.08e in the case of site B and larger than 0.1e in the case of site A. These values coincide exactly with the net positive charge on the acetonitrile molecule and correlate well with both the $\Delta\nu$(C≡N) vibration frequency shifts and the lengthening of the Sn–$O_{framework}$ bonds. This is so because the interaction between the active site and the Lewis base implies a lengthening of the four Sn–$O_{framework}$ distances, and this geometric change is considerably easier if one of the Sn–O–Si bridges of the active sites is hydrolysed.

The interaction of acetonitrile with the OH group of a Sn–O–H bridge has been calculated in one case, on site A-T9. As could be expected, the adsorption energy (−6.1 kcal/mol) is similar to that obtained for adsorption on a silanol group (−6.5 kcal/mol) and lower than that obtained for adsorption on the tin atom (−9.2 kcal/mol). The N–H distance is 1.927 Å and the lengthening of the CN bond is −0.003 Å, considerably smaller than that caused by adsorption of acetonitrile on the Sn atom (−0.007 Å). In correlation with these results, the shift in the ν(C≡N) vibration frequency of acetonitrile when it interacts with OH in the Sn–O–H group is 17 cm^{-1}, similar to that obtained for adsorption on silanol groups.

For a better comparison with experimental data, the geometries of the six adsorption complexes depicted in Fig. 1 were completely reoptimised at the highest theoretical level (DFT), and the $\Delta\nu$(C≡N) frequency shifts for these new structures were calculated. In Table 2, an average of the three values calculated for each type of site is given together with the IR measurements.

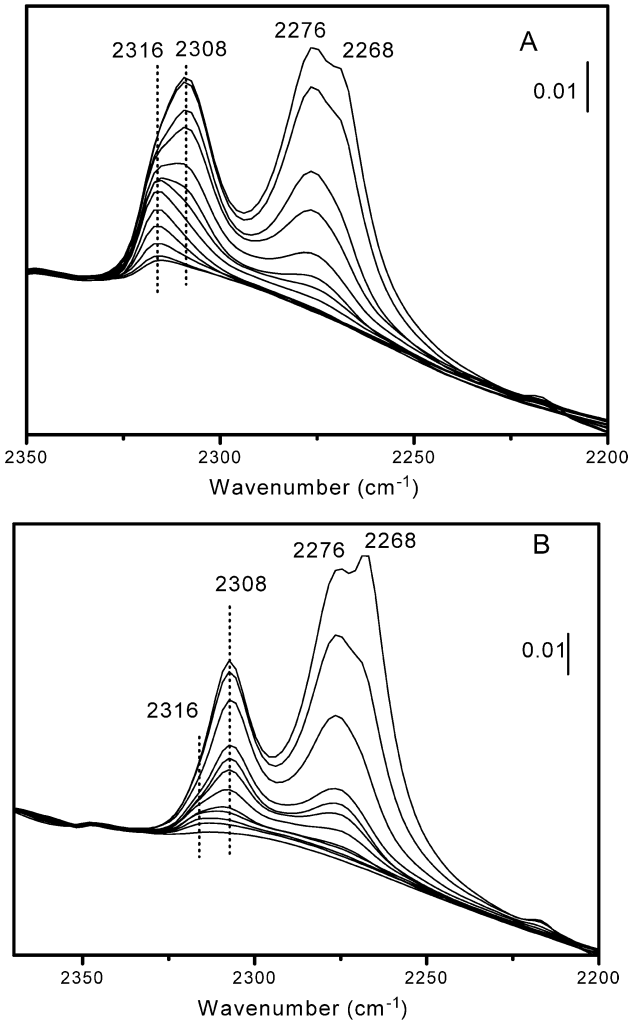

Fig. 3. IR spectra at increasing acetonitrile coverage on (a) 1SnB and (b) 2SnB_c samples.

3.2. IR experimental results

When deuterated acetonitrile was adsorbed on calcined Sn-beta, several bands in the 2260–2340 cm^{-1} IR region associated with ν(C≡N) stretching vibration can be observed. A weak band also appears at 2116 cm^{-1} that is due to δs(CD_3) vibration. In Fig. 3 the IR spectra in the

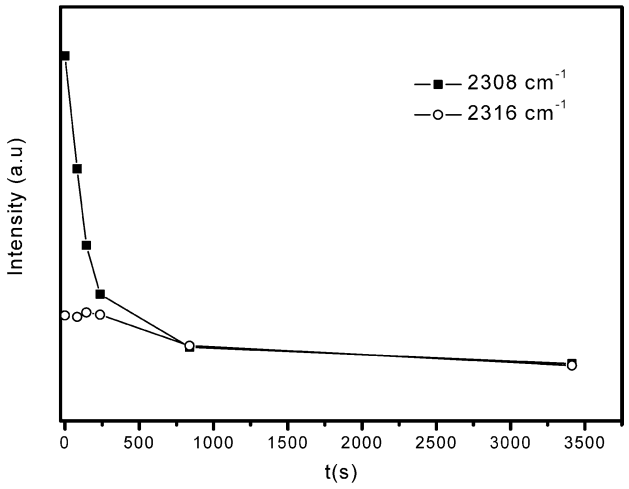

Fig. 4. Decrease of the intensity of the 2316 and 2308 cm^{-1} IR bands with time of desorption.

ν(C≡N) stretching vibration IR region are shown for two Sn-beta samples (1SnB and 2SnB_c). Four bands at 2316, 2308, 2276, and 2268 cm^{-1} are observed, and no shift in the band maxima occurs when acetonitrile coverage is increased. Bands at 2316 and 2308 cm^{-1} are associated with acetonitrile coordinated with Lewis acid sites [27,29], and IR bands at 2276 and 2268 cm^{-1} are due to acetonitrile coordinated to silanol groups and physisorbed acetonitrile, respectively. It should be noticed again that highly dispersed SnO_2 on pure silica beta, deposited by either CVD or by impregnation, does not show the 2316 and 2308 cm^{-1} IR bands when adsorbing acetonitrile.

The fact that there are two bands already indicates that two different types of Lewis acids sites must exist, and the higher relative shift of the band allows us to conclude that one of them interacts more strongly with acetonitrile (2316 cm^{-1} IR band) than the other (2308 cm^{-1} IR band). This was confirmed by the kinetics of acetonitrile desorption at 25 °C and 10^{-4} Torr, followed by IR spectroscopy. Indeed, results in Fig. 4 clearly show a much faster desorption of acetonitrile on sites responsible for the 2308 cm^{-1} band than for the 2316 cm^{-1} band.

With the IR results in hand, if we now establish a parallelism between the spectroscopy and theoretical results, we could associate the framework sites interacting more strongly with acetonitrile, which give a shift in the IR band of 51 cm^{-1}, with site A that involves partially hydrolysed framework Sn (Table 2). On the other hand, the Sn sites interacting less strongly with acetonitrile, and giving a shift in the IR band of 43 cm^{-1} should correspond to site B. It can be seen in Table 2 that ONIOM calculations already give the right tendency for the $\Delta\nu$(C≡N) shifts, but that the higher level DFT calculations exactly match the $\Delta\nu$(C≡N) shifts observed experimentally. This excellent agreement strongly supports the presence of sites A and B in Sn-beta zeolite.

The ν(OH) stretching vibration frequencies for the Si–OH and Sn–OH groups and the shift caused by interaction with acetonitrile were also calculated at the ONIOM level. The two values for the free catalyst are similar, 3765 and 3737 cm^{-1}, respectively. The shift in the ν(OH) frequency caused by the adsorption of acetonitrile on the silanol group is large, −238 cm^{-1}, and could be observed in the experimental IR spectrum. The shift calculated for the adsorption of acetonitrile on the tin center is only −30 cm^{-1}. Because of the low concentration of Sn–O–H sites and the small shift in the ν(OH) frequency, the Sn–O–H band could not be assigned unambiguously in the experimental IR spectrum.

3.3. Catalytic reactivity and maximisation of the number of active sites

Having in mind their related structures, it should be possible to change the relative population of sites A and B by postsynthesis treatments. Indeed, by calcination with air in an either dry or wet atmosphere, or by calcination in either a deep or a shallow bed [31], it should be possible to produce different levels of partially hydrolysed framework Sn sites.

In Table 3 we present a series of Sn-beta zeolites, with different Sn contents and subjected to different postsynthesis treatments. In the same table the ν(C≡N) IR band intensity associated with site A (2316 cm^{-1}) and site B (2308 cm^{-1}) upon adsorption of deuterated acetonitrile are given. Thus if one plots the initial rate for the oxidation of adamantanone to

Table 3
Calcination conditions of Sn Beta catalysts, and intensity of the 2316 and 2308 cm^{-1} IR bands

Sample	Sn (wt%)	Calcination	IR bands	
			2316 cm^{-1}	2308 cm^{-1}
1SnB	1	Furnance, 580 °C	0.0177	0.0751
2SnB	2	Furnance, 580 °C	0.0237	0.114
2SnB_a	2	Reactor, wet air[a], 580 °C, 500 mg, 280 ml/min	0.0125	0.104
2SnB_b	2	Reactor, dry air, 580 °C, 500 mg, 1000 ml/min	0.00664	0.107
2SnB_c	2	Reactor, dry air, 580 °C, 150 mg, 20 ml/min	0.000877	0.127
2SnB_d	2	Reactor, static[b], 580 °C, 600 mg	0	0.0522
2SnB_e	2	Reactor, static[b], 600 °C, 300 mg	0.0177	0.0751

[a] 4.2% of water.
[b] No gas flow was applied to the sample during calcination.

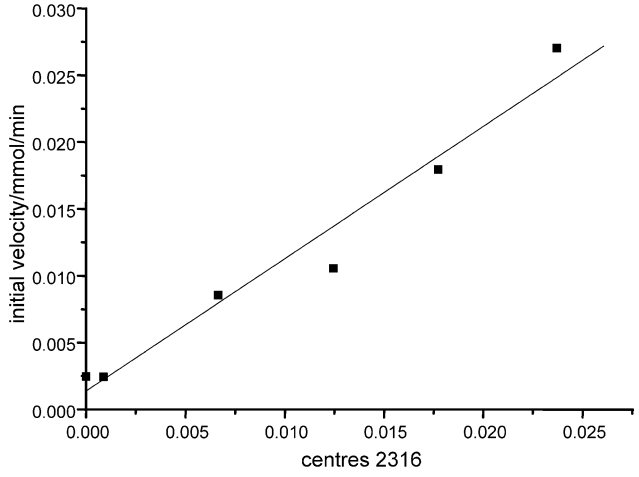

Fig. 5. Initial rate of the adamantanone oxidation versus intensity of the 2316 cm^{-1} IR band.

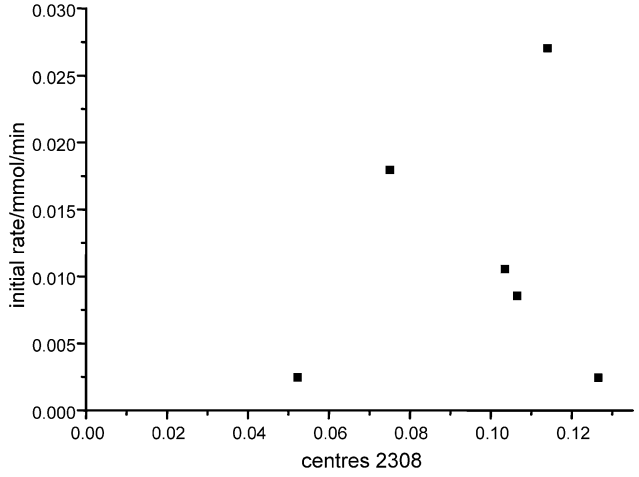

Fig. 6. Initial rate of the adamantanone oxidation versus intensity of the 2308 cm^{-1} IR band.

the corresponding lactone (Eq. (1)) versus the intensity of the two IR bands from Table 3, it is possible to see that a linear correlation is only observed with the intensity of the IR band at 2316 cm^{-1}, which corresponds with site A (Fig. 5) and not for the IR band at 2308 cm^{-1} (Fig. 6).

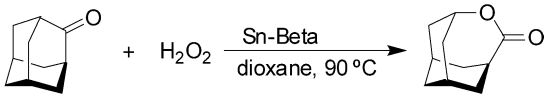

(1)

4. Conclusions

Two types of framework Sn sites in beta zeolite have been considered in the present work: partially hydrolysed and nonhydrolysed framework Sn, referred to as sites A and B, respectively.

Theoretical ONIOM and full DFT calculations for adsorbed acetonitrile (Lewis acid sites probe molecule) indicate that site A coordinates acetonitrile more strongly than site B. The DFT calculations predict two IR bands with shifts in the $\nu(C{\equiv}N)$ stretching vibration with respect to gas-phase acetonitrile of 43 and 53 cm^{-1}.

Experimental results for deuterated acetonitrile adsorption give two IR bands at 2316 and 2308 cm^{-1} for $\nu(C{\equiv}N)$, which represent IR shifts of 43 and 51 cm^{-1}, in excellent agreement with the theoretical simulations. This indicates that it is possible to measure the relative concentrations of sites A and B by deuterated acetonitrile adsorption.

By different postsynthesis treatments, catalysts with different concentrations of sites A and B were prepared. Catalytic results show that partially hydrolysed framework Sn sites (A) are much more active than fully framework integrated Sn (B) for Baeyer–Villiger oxidation of ketones, in perfect agreement with the better coordination abilities of these species.

Acknowledgments

The authors thank CICYT (MAT2003-07945-C02-01) for financing this work and the Universitat de Valencia for computing facilities. M.R. is grateful to the Spanish Ministry of Science and Technology for a “Ramón y Cajal” Fellowship.

References

[1] A. Corma, L.T. Nemeth, M. Renz, S. Valencia, Nature 412 (2001) 423.
[2] M. Renz, T. Blasco, A. Corma, V. Fornés, R. Jensen, L. Nemeth, Chem. Eur. J. 8 (2002) 4708.
[3] A. Corma, V. Fornés, S. Iborra, M. Mifsud, M. Renz, J. Catal. 221 (2004) 67.
[4] A. Corma, S. Iborra, M. Mifsud, M. Renz, M. Susarte, Adv. Synth. Catal. 346 (2004) 257.
[5] A. Corma, M.E. Domine, L. Nemeth, S. Valencia, J. Am. Chem. Soc. 124 (2002) 3194.
[6] A. Corma, M.E. Domine, S. Valencia, J. Catal. 215 (2003) 294.
[7] A. Corma, M. Renz, Chem. Commun. (2004) 550.
[8] R.R. Sever, T.W. Root, J. Phys. Chem. B 107 (2003) 10848.
[9] M. Boronat, A. Corma, M. Renz, G. Sastre, P.M. Viruela, Chem. Eur. J., in press.
[10] A. Carati, C. Flego, E. Massara, E. Previde, R. Millini, L. Carluccio, W.O. Parker Jr., G. Bellussi, Micropor. Mesopor. Mater. 30 (1999) 137.
[11] A. Zecchina, S. Bordiga, C. Lamberti, G. Ricchiardi, D. Scarano, G. Petrini, G. Leofanti, Catal. Today 32 (1996) 97.
[12] D. Gleeson, G. Sankar, C.R.A. Catlow, J.M. Thomas, G. Spano, S. Bordiga, A. Zecchina, C. Lamberti, Phys. Chem. Chem. Phys. 2 (2000) 4812.
[13] D.H. Wells Jr., W.N. Delgass, K.T. Thomson, J. Am. Chem. Soc. 126 (2004) 2956.
[14] J.M. Newsam, M.M.J. Treacy, W.T. Koetsier, C.B. de Gruyter, Proc. R. Soc. Lond. A 420 (1988) 375.
[15] M. Svensson, S. Humbel, R.D.J. Froese, T. Matsubara, S. Sieber, K. Morokuma, J. Phys. Chem. 100 (1996) 19357.
[16] S. Humbel, S. Sieber, K. Morokuma, J. Chem. Phys. 105 (1996) 1959.
[17] M.J. Frisch, G.W. Trucks, H.B. Schlegel, G.E. Scuseria, M.A. Robb, J.R. Cheeseman, J.A. Montgomery Jr., T. Vreven, K.N. Kudin, J.C. Burant, J.M. Millam, S.S. Iyengar, J. Tomasi, V. Barone, B. Mennucci, M. Cossi, G. Scalmani, N. Rega, G.A. Petersson, H. Nakatsuji, M. Hada, M. Ehara, K. Toyota, R. Fukuda, J. Hasegawa, M. Ishida, T. Nakajima, Y. Honda, O. Kitao, H. Nakai, M. Klene, X. Li, J.E. Knox, H.P. Hratchian, J.B. Cross, C. Adamo, J. Jaramillo, R. Gomperts, R.E. Stratmann, O. Yazyev, A.J. Austin, R. Cammi, C. Pomelli, J.W. Ochterski, P.Y. Ayala, K. Morokuma, G.A. Voth,

P. Salvador, J.J. Dannenberg, V.G. Zakrzewski, S. Dapprich, A.D. Daniels, M.C. Strain, O. Farkas, D.K. Malick, A.D. Rabuck, K. Raghavachari, J.B. Foresman, J.V. Ortiz, Q. Cui, A.G. Baboul, S. Clifford, J. Cioslowski, B.B. Stefanov, G. Liu, A. Liashenko, P. Piskorz, I. Komaromi, R.L. Martin, D.J. Fox, T. Keith, M.A. Al-Laham, C.Y. Peng, A. Nanayakkara, M. Challacombe, P.M.W. Gill, B. Johnson, W. Chen, M.W. Wong, C. Gonzalez, J.A. Pople, Gaussian 03, Revision B.04, Gaussian, Inc., Pittsburgh, PA, 2003.
[18] J.P. Perdew, Y. Wang, Phys. Rev. B 45 (1992) 13244.
[19] A.D. Becke, J. Chem. Phys. 98 (1993) 5648.
[20] W.R. Wadt, P.J. Hay, J. Chem. Phys. 82 (1985) 284.
[21] P.C. Hariharan, J.A. Pople, Theor. Chim. Acta 28 (1973) 213.
[22] A.P. Scott, L. Radom, J. Phys. Chem. 100 (1996) 16502.
[23] E.D. Glendening, A.E. Reed, J.E. Carpenter, F. Weinhold, NBO Version 3.1.
[24] S. Valencia, A. Corma, US Patent 5968473A (1999), to UOP LCC.
[25] OriginPro 7.5. http://www.originlab.com.
[26] J. Jänchen, G. Vorbeck, H. Stach, B. Parlitz, J.H.C. van Hooff, Stud. Surf. Sci. Catal. 94 (1995) 108.
[27] A.G. Pelmenschikov, R.A. van Santen, J. Jänchen, E. Meijer, J. Phys. Chem. 97 (1993) 11071.
[28] J. Chen, J.M. Thomas, G. Sankar, J. Chem. Soc. Faraday Trans. 90 (1994) 3455.
[29] B. Wichterlova, Z. Tvaruzkova, Z. Sobalik, P. Sarv, Micropor. Mesopor. Mater. 24 (1998) 223.
[30] L. Nemeth, J. Moscoso, N. Erdman, S.R. Bare, A. Oroskar, S.D. Kelly, A. Corma, S. Valencia, M. Renz, 14th International Zeolite Conference, South Africa, 2004, p. 2626.
[31] C.V. McDaniel, P.K. Maher, in: J.A. Rabo (Ed.), Zeolite Chemistry and Catalysis, ACS, Washington, DC, 1976, p. 320.